

Reversing Hydrology: Temporal aggregation and catchment rainfall estimation using sub-hourly data

1 **Reversing Hydrology: quantifying the temporal aggregation effect of catchment**
2 **rainfall estimation using sub-hourly data**

3

4 Quantifying temporal aggregation effects of catchment rainfall estimation

5

6 **Authors**

7 Kretzschmar, A¹., Tych, W^{1*}., Chappell, N.A¹., Beven, K.J.^{1,2}

8 ¹ Lancaster Environment Centre, Lancaster University, Lancaster LA1 4YQ, UK

9 ² Department of Earth Sciences, Uppsala University, Uppsala, Sweden

10

11 Corresponding author:

12 Dr. W. Tych,

13 Lancaster Environment Centre,

14 Lancaster University,

15 Lancaster

16 LA1 4YQ,

17 UK

18 w.tych@lancaster.ac.uk

19 +44 (0)1524 593973

20

21 **Abstract**

22 Inferred rainfall sequences generated by a novel method of inverting a continuous

23 time transfer function show a smoothed profile when compared to the observed

24 rainfall however streamflow generated using the inferred rainfall is almost identical to

25 that generated using the observed rainfall ($R_t^2 = 95\%$). This paper compares the

Reversing Hydrology: Temporal aggregation and catchment rainfall estimation using sub-hourly data

26 inferred effective and observed effective rainfall in both time and frequency domains
27 in order to confirm that, by using the dominant catchment dynamics in the inversion
28 process, the main characteristics of catchment rainfall are being captured by the
29 inferred effective rainfall estimates. Estimates of the resolution of the inferred
30 effective rainfall are found in the time domain by comparison with aggregated
31 sequences of observed effective rainfall, and in the frequency domain
32 by comparing the amplitude spectra of observed and inferred effective rainfall. The
33 resolution of the rainfall estimates is affected by the slow time constant of the
34 catchment and the rainfall regime, but also by the goodness-of-fit of the model, which
35 incorporates the amount of other disturbances in the data.

36 **Keywords**

37 Continuous time; data based mechanistic modelling; time resolution; spectral
38 analysis; reverse hydrology; transfer function;

39 **Introduction**

40 Rainfall is the key driver of catchment processes and is usually the main input to
41 rainfall-streamflow models. If the rainfall and/or streamflow data used to identify or
42 calibrate a model are wrong or disinformative, the model will be wrong and cannot be
43 used to predict the future with any certainty. Bloeschl *et al.* (2013) state that if the
44 dominant pathways, storage and time-scales of a catchment are well defined then a
45 model should potentially reproduce the catchment dynamics under a range of
46 conditions. It is often the case that hydrological variables, such as rainfall and
47 streamflow, are measured at hourly or sub-hourly intervals then aggregated up to a
48 coarser resolution before being used as input to rainfall-streamflow models
49 resulting in the loss of information about the finer detail of the catchment processes
50 (Littlewood and Croke, 2008; Littlewood *et al.*, 2010; Littlewood and Croke, 2013).

51 Kretzschmar *et al.* (2014) have proposed a method for inferring catchment rainfall
52 using sub-hourly streamflow data. The resulting rainfall record is smoothed to a
53 coarser resolution than the original data but should still retain the most pertinent
54 information.

55 This paper investigates the implications of the reduced resolution and the
56 potential loss of information introduced by the regularisation process in both the time
57 and frequency domains. Both temporal and spatial aggregation are incorporated in the
58 transfer function model however only the temporal aspect is considered here. The
59 effect of spatial rainfall distribution using sub-catchments will be the subject of a
60 future publication.

61 The method developed and tested by Kretzschmar *et al.* (2014) – termed the
62 RegDer method - inverts a continuous-time transfer function (CT-TF) model using a
63 regularised derivative technique to infer catchment rainfall from streamflow with the
64 aim of improving estimates of catchment rainfall arguing that a model that is well-
65 fitting and invertible is likely to be robust in terms of replicating the catchment
66 system.

67 The classical approach to inverse (as opposed to reverse) modelling involves
68 the estimation of non-linearity (rainfall or baseflow separation) and the unit
69 hydrograph (UH), which is an approximation to the impulse response of the
70 catchment. Boorman (1989) and Chapman (1996) use sets of event hydrographs to
71 estimate the catchment UH. Boorman (1989) superimposed event data before
72 applying a separation technique and concluded that the data required may be more
73 coarsely sampled than might be expected because one rain-gauge is unlikely to be
74 representative of the whole catchment. Chapman (1996) used an iterative procedure
75 to infer rainfall patterns for individual events before applying baseflow separation.

76 The resultant UHs had higher peaks and shorter rise times and durations than those
77 obtained by conventional methods. He viewed the effective rainfall as the output from
78 a non-linear store. Duband *et al.* (1993) and Olivera and Maidment (1999) used
79 deconvolution to identify mean catchment effective rainfall which was redistributed using
80 relative runoff coefficients whilst Young and Beven (1994) based a method for inferring
81 effective rainfall patterns on the identification of a linear transfer function. A gain
82 parameter, varying with time accounted for the non-linearity in the relationship between
83 rainfall and streamflow.

84 In recent years, a range of different approaches has been used to explore
85 reverse modelling in hydrology, that is, estimating effective rainfall from streamflow.
86 Notable publications include Croke (2006), Kirchner (2009), Andrews and Croke
87 (2010), Young and Sumislawska (2012), Brocca *et al.* (2013, 2014) and Kretzschmar
88 *et al.* (2014). Kirchner's method links rainfall, evapo-transpiration and streamflow
89 through a sensitivity function making assumptions which allow rainfall to be inferred
90 from the catchment streamflow. The method has been applied by Teuling *et al.* (2010)
91 and Krier *et al.* (2012) to catchments in Switzerland and Luxembourg and has been
92 found to work for catchments with simple storage-streamflow relationships and
93 limited hysteresis. Brocca *et al.* (2013) employed a similar method based on the water
94 balance equation but inferred the rainfall series from soil moisture. In a further study,
95 Brocca *et al.* (2014) used satellite derived soil moisture to infer global rainfall
96 estimates. Croke (2006) derived an event-based unit hydrograph from streamflow
97 alone but his approach was limited to ephemeral quick-flow-dominant catchments
98 whilst Andrews *et al.* (2010) and Young and Sumislawska (2012) use a discrete
99 model formulation inverted directly or via a feedback model (which could be adapted
100 to CT formulation). The approach proposed by Kretzschmar *et al.* (2014) combined a

Reversing Hydrology: Temporal aggregation and catchment rainfall estimation using sub-hourly data

101 continuous time transfer function (CT-TF) model with regularized derivative
102 estimates to infer the catchment rainfall from sub-hourly streamflow data.

103 Littlewood (2007) applied the IHACRES model (e.g. Jakeman *et al.*, 1990) to
104 the River Wye gauged at Cefn Brwyn showing that the values for the model
105 parameters for that catchment changed substantially as the data time step used for
106 model calibration decreased. Littlewood and Croke (2008) extended this work to
107 include a second catchment and found that as the time-step decreased the parameter
108 values approached an asymptotic level (on a semi-log plot) concluding that, at small
109 enough time-steps, parameters become independent of the sampling interval. They
110 suggested further investigation using data-based mechanistic modelling (DBM)
111 methods as described by Young and Romanowicz (2004) and Young and Garnier
112 (2006) for estimating CT models from discrete input data. Such models generate
113 parameter values independent of the input sampling rate – as long as the sampling rate
114 is sufficiently high in comparison to the dominant dynamics of the system.
115 Advantages of using the CT formulation include allowing a much larger range of
116 system dynamics to be modelled e.g. ‘stiff’ systems that have a wide range of time-
117 constants (TC), typical of many hydrological systems. The outputs from such a model
118 can be sampled at any time-step, including non-integer, and the parameters have a
119 direct physical interpretation (Young, 2010).

120 Krajewski *et al.* (1991) compared the results from a semi-distributed model
121 and a lumped model and concluded that catchment response is more sensitive to
122 rainfall resolution in time than space whilst a study by Holman-Dodds *et al.* (1999)
123 demonstrated that models calibrated using a smoothed rainfall signal (due to coarse
124 sampling) may result in under-estimation of streamflow. Further calibration, required
125 to compensate, leads to the loss of physical meaning of parameters. They also

126 concluded that parameters estimated at one sampling interval were not transferable to
127 other intervals; a conclusion echoed by Littlewood (2007) and Littlewood and Croke
128 (2008).

129 Studies by Clark and Kavetski (2010) showed that in some cases, numerical
130 errors due to the time-step are larger than model structural errors and can even
131 balance them out to produce good results. The follow-up study by Kavetski and Clark
132 (2010) looked at its impact on sensitivity analysis, parameter optimisation and Monte
133 Carlo uncertainty analysis. They concluded that use of an inappropriate time step can
134 lead to erroneous and inconsistent estimates of model parameters and obscure the
135 identification of hydrological processes and catchment behaviour. Littlewood and
136 Croke (2013) found that a discrete model using daily data over-estimated time-
137 constants for the River Wye gauged at Cefn Brwyn when compared to those estimated
138 from hourly data confirming that parameter values were dependent on the time-step.
139 They discussed the loss of information due to the effect of time-step on time constants
140 and suggested that plots of parameter values against time step could be used as a
141 model assessment tool. In a previous study, Littlewood and Croke (2008), compared
142 the sensitivity of parameters for two catchments with respect of time-step and
143 discussed the role of time-step dependency on the reduction of uncertainty. They also
144 suggested continuous time transfer function modelling using sub-hourly data to derive
145 sampling rate independent parameter values. Littlewood *et al.* (2010) introduced the
146 concept of the Nyquist-Shannon (N-S) sampling theorem, which defines the upper
147 bound on the size of sampling interval required to identify the CT signal without
148 aliasing, and consequentially its effect on the frequency of sampling required to
149 specify a rainfall-streamflow model. Given a frequent enough sampling rate, the CT
150 model is time independent and can be interpreted at any interval.

151 Further understanding may be gained by transforming rainfall and streamflow
152 series from the time domain to the frequency domain and using spectral analysis.
153 Several potential uses of spectral analysis in hydrology have been explored including
154 modelling ungauged catchments, modelling karst systems and seasonal adjustment of
155 hydrological data series. A maximum likelihood method for model calibration based
156 on the spectral density function (SDF) has been suggested by Montanari and Toth
157 (2007). The SDF can be inferred from sparse historic records in the absence of other
158 suitable data making it a potentially useful tool for modelling ungauged catchments.
159 They also suggest that spectral analysis may provide a means of choosing between
160 different apparently behavioural models. Cuchi *et al.* (2014) used ‘black box’
161 modelling and frequency analysis to study the behaviour of a karst system (located at
162 Fuenmajor, Huesca, Spain). They concluded that method works well for a linear
163 system and that Fuenmajor has a linear hydrological response to rainfall at all except
164 high frequencies. They suggest that the non-linearity issues might be addressed using
165 appropriate techniques such as wavelets or neural networks. Szolgayova *et al.* (2014)
166 utilised wavelets to deseasonalise a hydrological time-series and suggested that the
167 technique had potential for modelling series showing long term dependency
168 (interpreted as containing low frequency components).

169 The method introduced by Kretzschmar *et al.* (2014) showed that given that
170 the rainfall-streamflow model captures the dynamics of the catchment system, the
171 high frequency detail of the rainfall distribution is not necessary for the prediction of
172 streamflow due to the damping (or low-pass filter) effect of the catchment response.
173 The regularisation process introduced is numerically stable at the cost of a loss of
174 some temporal resolution in the inferred rainfall time series. The regularisation level
175 is controlled through the Noise Variance Ratio (NVR), optimised as part of the

176 process and is only applied when necessary, i.e. when the analytically inverted
177 catchment transfer function model is improper (has a numerator order higher than the
178 denominator order).

179 **Application catchments**

180 RegDer has been tested on two headwater catchments with widely differing rainfall
181 and response characteristics – Baru in humid, tropical Borneo and Blind Beck, in
182 humid temperate UK. The 0.44 km² Baru catchment is situated in the headwaters of
183 the Segama river on the northern tip of Borneo, East Malaysia. The climate is
184 equatorial showing no marked seasonality but tending to fall in short (<15 min)
185 convective events showing high spatial variability and intensities much higher than
186 those of temperate UK (Bidin and Chappell, 2003, 2006). Haplic alisols, typically 1.5
187 m in depth and with a high infiltration capacity (Chappell *et al.*, 1998) are underlain
188 by relatively impermeable mudstone bedrock resulting in the dominance of
189 comparatively shallow sub-surface pathways in this basin (Chappell *et al.*, 2006). As
190 a result of the high rainfall intensity and shallow water pathways the stream response
191 is very flashy. In contrast, the Blind Beck catchment has an area of 8.8 km² and its
192 response shows evidence of deep hydrological pathways due to the presence of deep
193 limestone and sandstone aquifers resulting in a damped hydrograph response (Mayes
194 *et al.*, 2006; Ockenden and Chappell, 2011; Ockenden *et al.*, 2014). Winter rainfall in
195 this basin is derived from frontal systems with typically lower intensities than the
196 convective systems in Borneo (Reynard and Stewart, 1993).

197 **Model formulation and physical interpretation**

198 This study investigated the limits of inferred catchment effective rainfall estimation
199 from streamflow. Continuous time transfer function models identified from the
200 observed data using Data Based Mechanistic (DBM) modelling approaches (Young

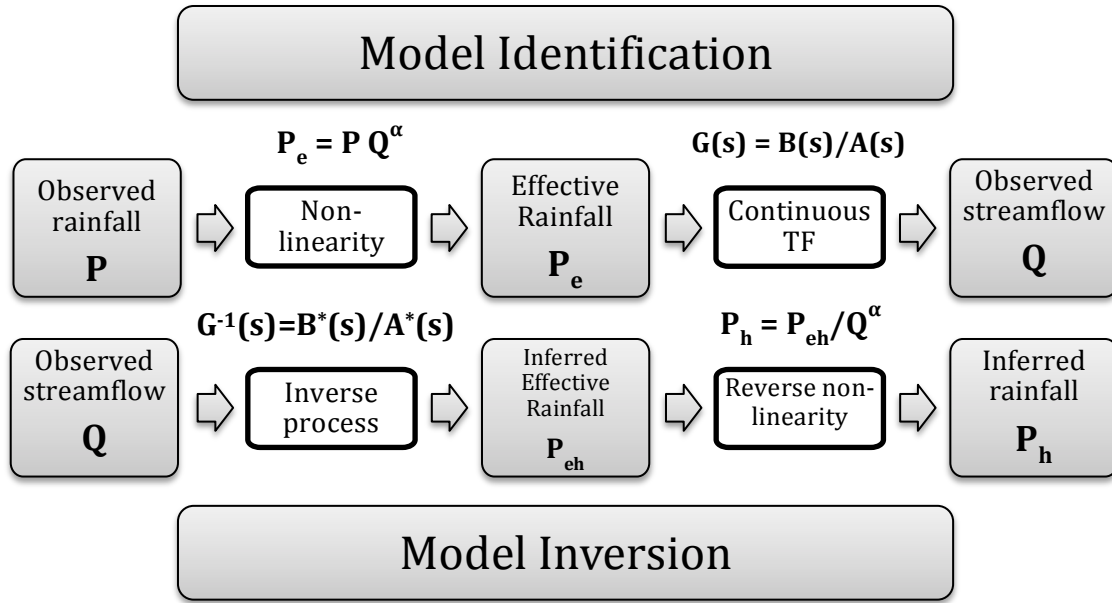
201 and Beven, 1994; Young and Garnier, 2006), are inverted using the RegDer method
202 (Kretzschmar *et al.*, 2014) and used to transform catchment streamflow into estimates
203 of catchment inferred rainfall.

204 DBM modelling makes no prior assumptions about the model structure
205 (though it often uses structures based on transfer functions), which is suggested by the
206 observed data, and must be capable of physical interpretation. As transfer functions
207 are linear operators, a transform structured as a bilinear power-law (Eq. (1)), also
208 identified from the observed data, was applied to linearise the data before model
209 fitting (Young and Beven, 1994; Beven, 2012, .p91):

$$210 \quad P_e = P Q^\alpha \quad (1)$$

212 where P is the observed rainfall, Q the observed streamflow and α is a parameter,
213 estimated from the data. P_e is the effective observed rainfall (ER) and Q is used as a
214 surrogate for catchment wetness. Both catchments used in this study proved to be
215 predominantly linear in their behaviour so transformation Eq. (1) was not used. In the
216 initial study, a wide range of possible models was identified using algorithms from
217 the Captain Toolbox for Matlab (Taylor *et al.*, 2007). The models selected were a
218 good fit to the data and were suitable for inversion. The Nash-Sutcliffe Efficiency
219 (NSE or R_t^2) is commonly used to compare the performance of hydrological models.
220 Often several models can be identified that fit the data well (the equifinality concept
221 of Beven, 2006). From these, models with few parameters to be estimated that
222 inverted well were selected. In this study a second order linear model was found to fit
223 both catchments. The output from the RegDer process is an inferred effective rainfall
224 series to which the reverse of the power law is then applied, if necessary, to construct
225 an inferred catchment rainfall sequence. The process is illustrated in Fig. 1.

227



228

229

230

231

232

233

234

235

Figure 1 - model identification and inversion workflow where P is the observed catchment rainfall, P_e is the effective rainfall, Q is the observed streamflow, P_{eh} is the inferred effective rainfall and P_h the inferred catchment rainfall. Non-linearity is represented by the bilinear power law (Beven, 2012, p91). The continuous time transfer function is given by $G(s)$ where $A(s)$ and $B(s)$ are the denominator and numerator polynomials and the inversion process is represented by $G^{-1}(s)$ where $A^*(s)$ and $B^*(s)$ are the denominator and numerator polynomials of the inverted transfer function.

236

The transfer function model inversion process has been described in

237

Kretschmar *et al.* (2014). It involves transition from the transfer function catchment

238

model:

239

$$Q = G(s)R = \frac{\beta_0 s^m + \beta_1 s^{m-1} + \dots + \beta_m}{s^n + \alpha_1 s^{n-1} + \dots + \alpha_n} e^{-s\tau} P_e \quad (2)$$

240

to the direct inverse (in general non-realisable):

241

242

$$\hat{R} = \frac{b_0 s^n + b_1 s^{n-1} + \dots + b_n}{s^m + a_1 s^{m-1} + \dots + a_m} e^{s\tau} Q \quad (3)$$

243

which is then implemented using regularised streamflow derivatives in the form of:

244

245

$$\hat{R} e^{-s\tau} = \frac{b_0 \{s^n Q\}^* + b_1 \{s^{n-1} Q\}^* + \dots + b_n Q}{s^m + a_1 s^{m-1} + \dots + a_m} \quad (4)$$

246 where $\{\widehat{s^n Q}\}^* = \mathcal{L}\left\{\frac{d^n}{dt^n} Q\right\}$ is the Laplace transform of the optimised regularised
247 estimate of the n^{th} time derivative of Q : $\frac{d^n}{dt^n} Q$. The regularised derivative estimates
248 replace the higher order derivatives in Eq. (3), which otherwise make Eq. (3)
249 unrealisable (improper) – this is the core of the method in Kretzschmar *et al.* (2014).
250 In the implementation, n^{th} derivatives in Eq. (4) are not estimated, but advantage is
251 taken of the filtering with the denominator polynomial, and only $(n-m)^{\text{th}}$ derivative
252 estimates are required in combination with a proper transfer function.

253 The inferred effective rainfall (IR) sequences generated by RegDer generally
254 have a much smoother profile (illustrated in Fig. 2) than the observed rainfall inputs,
255 however streamflow sequences generated with the IR used as the model input are
256 almost indistinguishable from the sequence modelled using observed rainfall ($R_t^2 =$
257 95%). This indicates that the catchment dynamics, as captured by the transfer function
258 model, renders the differences between observed and inferred rainfall immaterial. The
259 reason for this becomes clear when looking at the frequency domain analysis of the
260 inversion process shown in this paper.

261 In order to investigate this, the IR is compared to aggregated effective
262 observed rainfall sequences with increasing levels of aggregation until a good match
263 is found (high value of R_t^2 or R). Two methods of aggregation have been used: 1)
264 averaging over a range of time-series, 2) moving average over varying time scales.
265 Two measures are used to assess the correspondence between the IR and the
266 aggregated effective rain: 1) R_t^2 , the coefficient of determination, and 2) R , the
267 instantaneous Pearson correlation coefficient. They are given by:

268
269
$$R_t^2 = 1 - \frac{\sum(ER-IR)^2}{\sum(ER-\overline{ER})^2} \quad (5a)$$

270

271

$$R = \frac{\sum(ER - \overline{ER})(IR - \overline{IR})}{\sqrt{\sum(ER - \overline{ER})^2} \sqrt{\sum(IR - \overline{IR})^2}} \quad (5b)$$

273

274 where ER indicates a value from the aggregated effective rainfall sequence with mean

275 \overline{ER} and IR is the corresponding value from the inferred effective rainfall sequence

276 with mean \overline{IR} . Both R_t^2 and R values tend towards a maximum value as aggregation

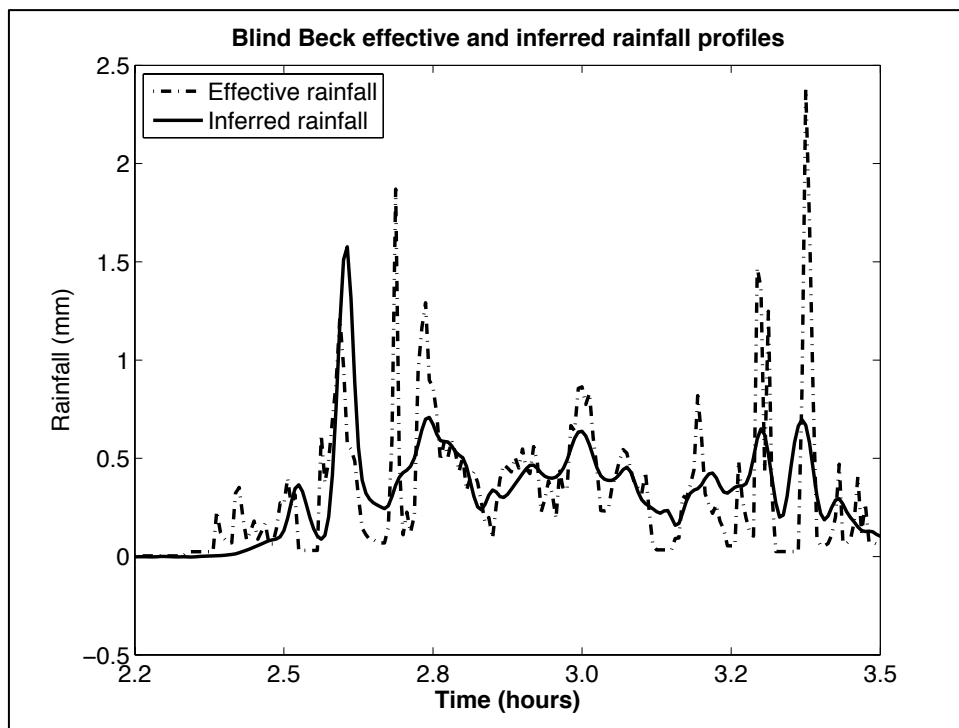
277 increases. The aggregation level at which the maximum is reached is identified and

278 taken as an estimate of the resolution of the inferred effective series. This value is

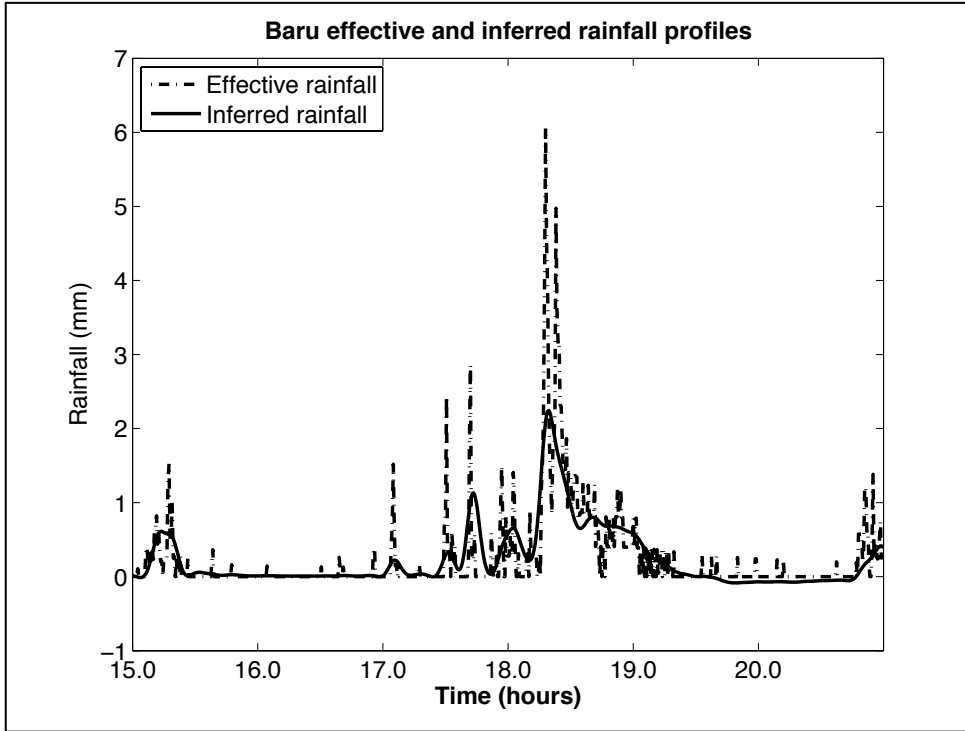
279 then compared to the system fast time constant (TC_q) and the Nyquist-Shannon (N-S)

280 sampling limit.

281



282 a)



283
284
285
286

b) Figure 2 – observed effective and inferred rainfall profiles generated using the RegDer inversion method for a) Blind Beck and b) Baru

287 Continuous model formulation

288 One of the advantages of using a CT model formulation is that the parameters have a
289 direct physical interpretation independent of the model's sampling rate (Young,
290 2010). The continuous time model formulation for a 2nd-order model is given by:

291
292
$$y(t) = \frac{\beta_0 s + \beta_1}{s^2 + \alpha_1 s + \alpha_2} u(t - \delta) \quad (6)$$

293
294 where y is the measured streamflow at time t , δ is the transport delay and u is the
295 effective rainfall at time $t - \delta$. If the denominator can be factorized and has real roots,

296 Eq. (6) can be rewritten as:

297
298
$$y(t) = \frac{\beta_0 s + \beta_1}{(s + \frac{1}{TC_q})(s + \frac{1}{TC_s})} u(t - \delta) \quad (7)$$

299
300 where TC_q and TC_s are the system time constants and are often significantly different
301 – a 'stiff' system. Decomposing the model into a parallel form gives:

302

$$303 \quad y(t) = \left(\frac{g_q}{1+TC_q s} + \frac{g_s}{1+TC_s s} \right) u(t - \delta) \quad (8)$$

304

305 where g_q and TC_q are the steady state gain and time constant of the fast response

306 component and g_s and TC_s are the steady state gain and time constant of the slow

307 response component. The steady state gain of the system as a whole is given by:

308

$$309 \quad g = g_q + g_s \quad (9)$$

310

311 so the fraction of the total streamflow along each pathway can be calculated from:

312

$$313 \quad P_q = \frac{g_q}{g_q + g_s}; P_s = \frac{g_s}{g_q + g_s} \quad (10)$$

314

315 The fraction of streamflow attributed to the slow response component is sometimes

316 termed the Slow Flow Index (SFI) (Littlewood *et al.*, 2010). The example shown here

317 uses a second order model but the general principle can be extended to higher order

318 models. Details of the inversion and regularisation processes can be found in

319 Kretzschmar *et al.* (2014).

320 **Sampling frequency**

321 When using CT modelling, the Nyquist-Shannon frequency gives the upper limit on

322 the size of the sampling interval, Δt , that will enable the system dynamics to be

323 represented without distortion (aliasing - Bloomfield, 1976, p21). Aliasing occurs

324 when a system is measured at an insufficient sampling rate to adequately define the

325 signal from the data.

326 The Nyquist-Shannon theorem states that the longest sampling step for a

327 signal with bandwidth Ω (maximum frequency, where $\Omega = 2\pi f$ in cycles per time

328 unit) to be represented is:

329

$$330 \quad \Delta t \leq \frac{1}{2\Omega} \quad (11)$$

331

332 in order to completely define the system in absence of observation disturbance
333 (Young, 2010). If the sampling interval is small enough to uniquely define the system,
334 the estimated CT model should be independent of the rate of sampling. Conversely, if
335 the frequency of the inferred output is less than the N-S limit, then the system
336 dynamics should be adequately captured. Other estimates of the sufficient sampling
337 interval, designed to avoid proximity to the Nyquist limit, have been made by Ljung
338 (1999) and Young (2010). In terms of system TCs, these limits are given by:

339
340
$$Nyquist = \pi TC_q \text{ time units} \quad (12a)$$

341
342
$$Ljung = \frac{\pi TC_q}{5} \text{ time units} \quad (12b)$$

343
344
$$Young = \frac{TC_q}{6} \text{ time units} \quad (12c)$$

345

346 **Temporal aggregation of effective rainfall**

347 Two methods for aggregating ER were used to estimate the time resolution of the IR.
348 Rainfall is the total volume accumulated over the sampling interval so the ER was
349 aggregated over progressively longer sampling periods of 2 to 24 times the base
350 sampling period and averaged to form a new smoothed sequence that could be
351 compared with the IR. For comparison, aggregation was also performed via a moving
352 average process utilising the convolution method available in Matlab. Both methods
353 may be affected by the aggregation starting point and edge effects. The aggregated
354 ER sequences were compared to the IR using the coefficient of determination (R_t^2)
355 and the correlation (R). R_t^2 and R tend towards a maximum value as aggregation
356 increases. The aggregation time-step at which this value is established is used to
357 estimate the resolution of the IR.

358 **Spectral Analysis**

359 Periodograms of the amplitude spectra of the observed and modelled series were
360 plotted to test whether the ER and IR have the same dynamics in the critical
361 frequency range, despite the loss of time resolution (related to low pass filtering due
362 to regularisation). A periodogram is the frequency domain representation of a signal;
363 transforming the signal into the frequency domain may reveal information that is not
364 visible in the time domain. A transfer function shown in its equivalent frequency
365 domain form describes the mapping between the input and the output signals' spectra
366 for the linear dynamic systems used here. Signals may be easily transformed
367 between the time and frequency domains (Wickert, 2013).

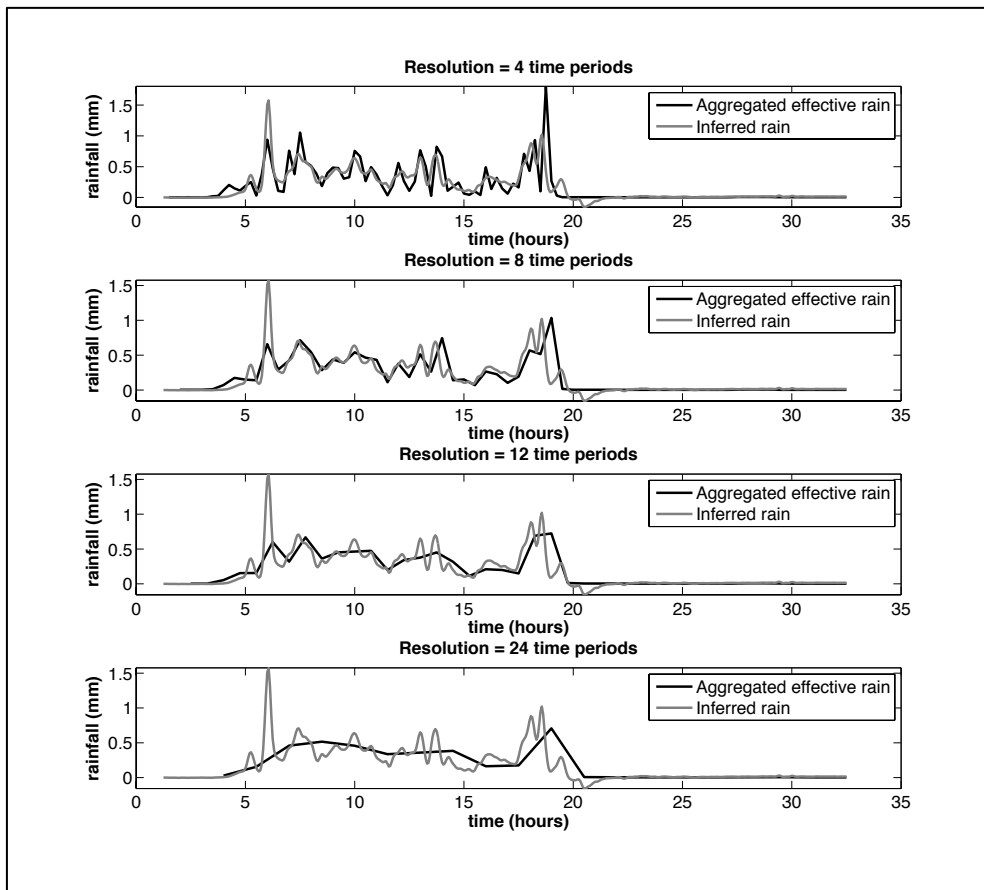
368 Periodograms are obtained using the Matlab implementation via the Fast
369 Fourier Transform and smoothed using the Integrated Random Walk (e.g. Young *et al.*
370 *al.*, 1999); the same regularisation approach as used in the calculation of the IR,
371 implemented in the Captain Toolbox (Taylor *et al.*, 2007). Periodograms of ER, IR
372 and catchment streamflow are compared on a single plot showing how the spectral
373 properties of the inversion process are used to obtain the IR estimates (see Fig. 6).
374 The streamflow spectrum is the result of mapping the rainfall spectrum by the
375 catchment dynamics. To make a full inversion of that mapping would involve very
376 strong amplification of high frequencies with all the negative consequences discussed
377 by Kretzschmar *et al.* (2014). The most significant implications of full inversion
378 include the introduction of high amplitude, high frequency noise artefacts into the
379 rainfall estimates. The regularisation of estimated derivatives introduces the effect of
380 low-pass filtering into the inversion process, avoiding the excessive high frequency
381 noise. Regularisation does not introduce any lag into the process, unlike traditional
382 low pass filtering.

383 **Results and discussion**

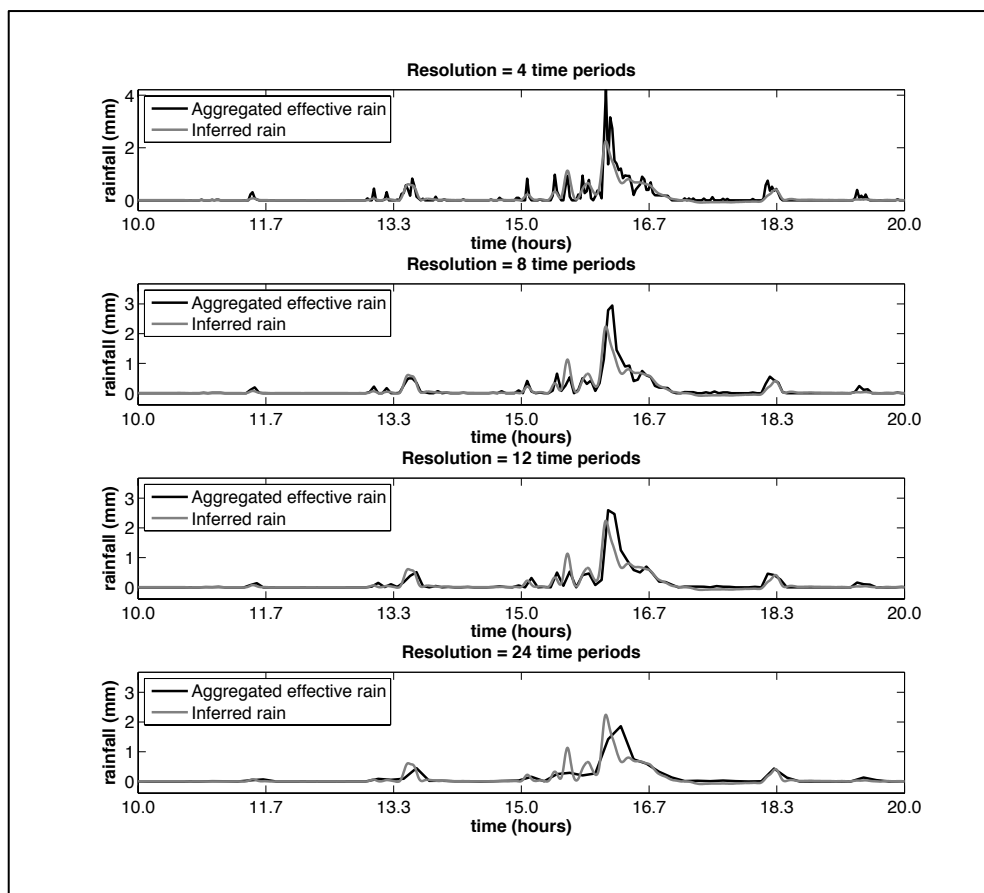
384 Fig. 2 illustrates the smoothed rainfall distribution of the IR sequence obtained using
385 the RegDer method. Similar streamflow sequences are generated using either the ER
386 or IR sequences as model input (see Kretzschmar *et al.*, 2014). The implication is that
387 the catchment system dynamics are being captured despite the apparent difference in
388 the rainfall distribution and that the detail of the rainfall series in time may not be
389 important when modelling the dominant mode of streamflow dynamics.

390 In order to assess the degree of resolution lost by estimating rainfall using the
391 RegDer method, the ER was aggregated using two methods (i.e. simple aggregation
392 by resampling and a moving average) and the resulting sequences compared to the IR
393 sequence in the time domain. Plots of progressively more aggregated sequences are
394 shown in Fig. 3. It can be seen that as aggregation increases, peaks become lower and
395 more spread out and the sequence is effectively smoothed. The coefficient of
396 determination (R_t^2) and the correlation (R) between the aggregated sequence and the
397 IR tends to a maximum then decreases as aggregation time increases – ultimately the
398 variation in the sequence would be completely smoothed out. The point at which the
399 maximum value is reached is taken as an estimate of the resolution of the IR. Plots of
400 R_t^2 or R values are shown in Fig. 4 (aggregation by resampling) and Fig. 5 (moving
401 average estimate). Time resolution estimates are shown in Table 1 and compared with
402 the fast time constant (TC_q) and the Nyquist-Shannon sampling limit.

Reversing Hydrology: Temporal aggregation and catchment rainfall estimation using sub-hourly data



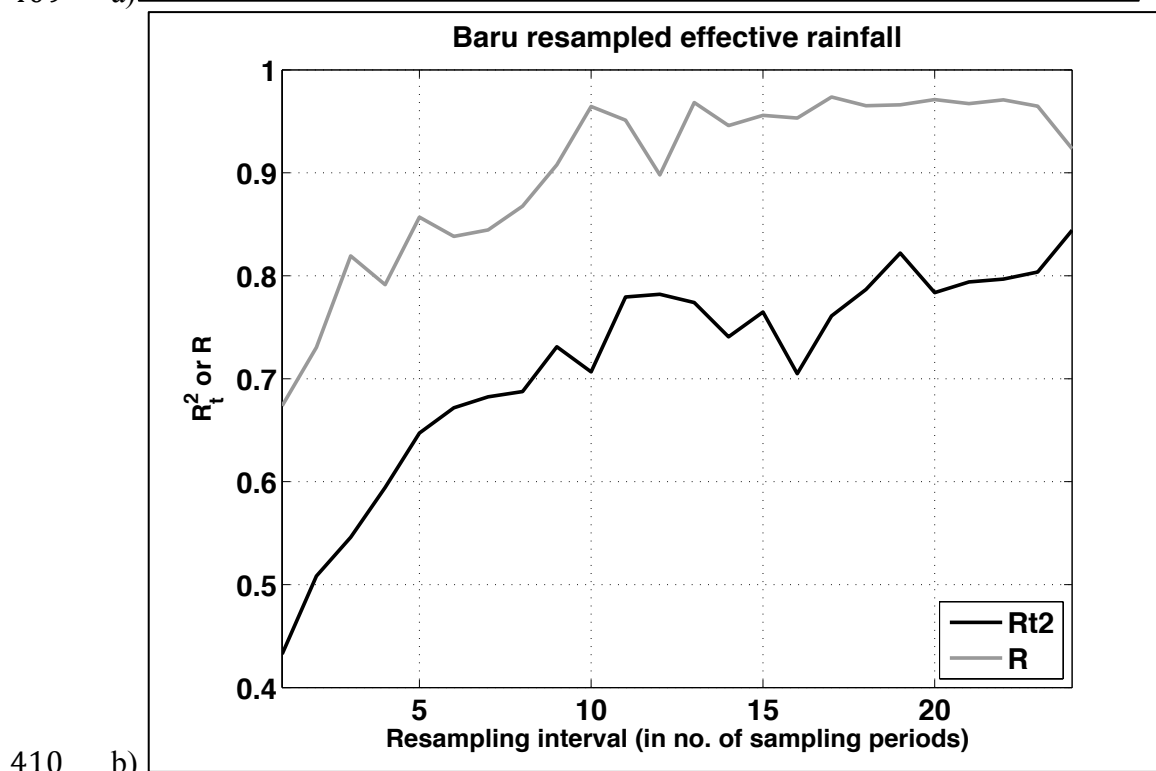
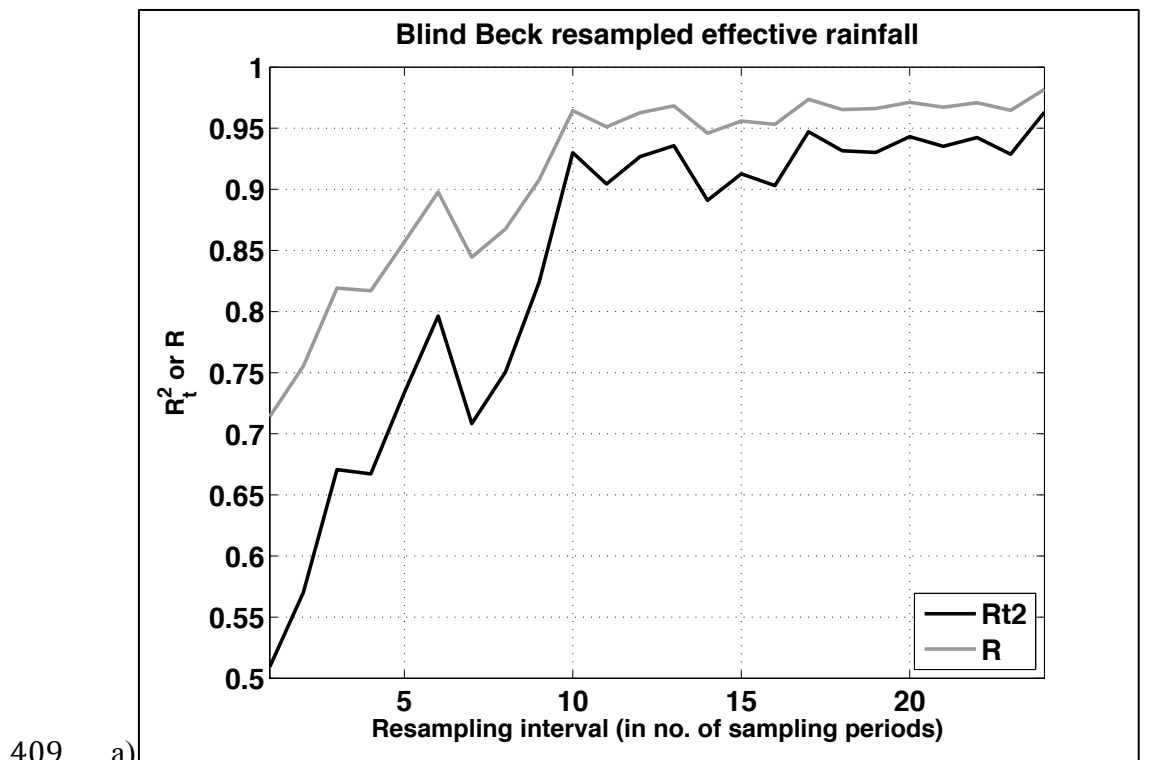
403 a)



404 b)

Reversing Hydrology: Temporal aggregation and catchment rainfall estimation using sub-hourly data

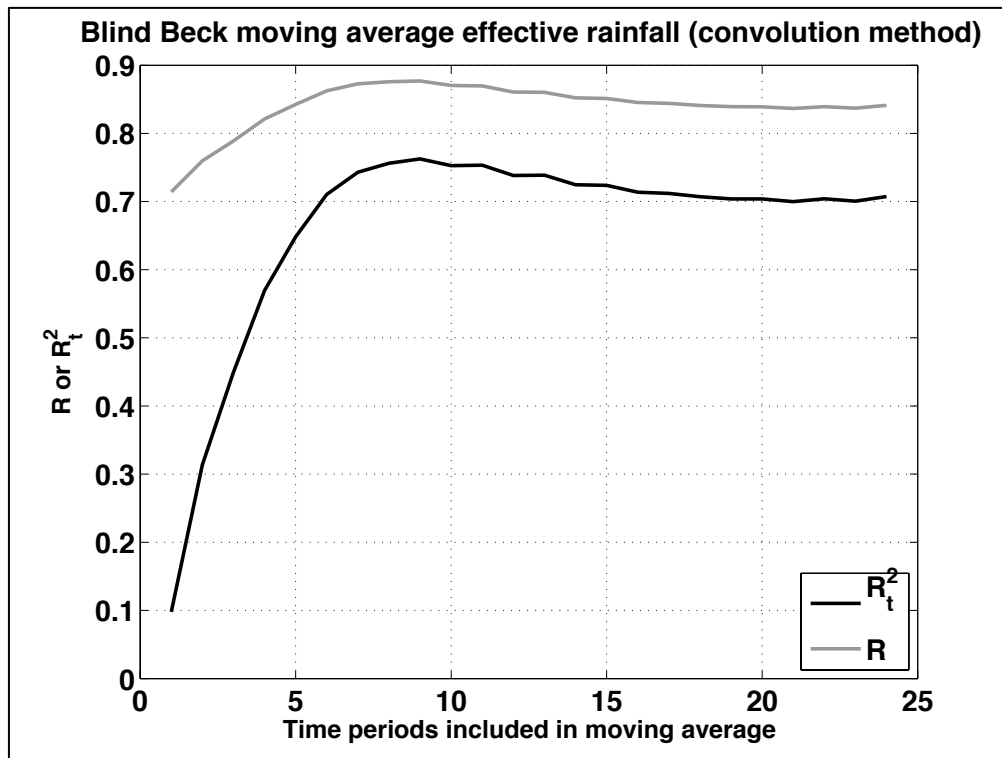
405 Figure 3 – Comparison of aggregated sequence to the Inferred effective rainfall sequence for a) Blind Beck
 406 (sampling interval 15 mins) b) Baru (sampling interval 5 mins) at aggregations of 4, 8 12 and 24 time periods
 407 illustrating how aggregation lowers the peak and spreads the volume of rainfall over a longer time period. The
 408 inferred effective rainfall sequence is plotted for comparison.



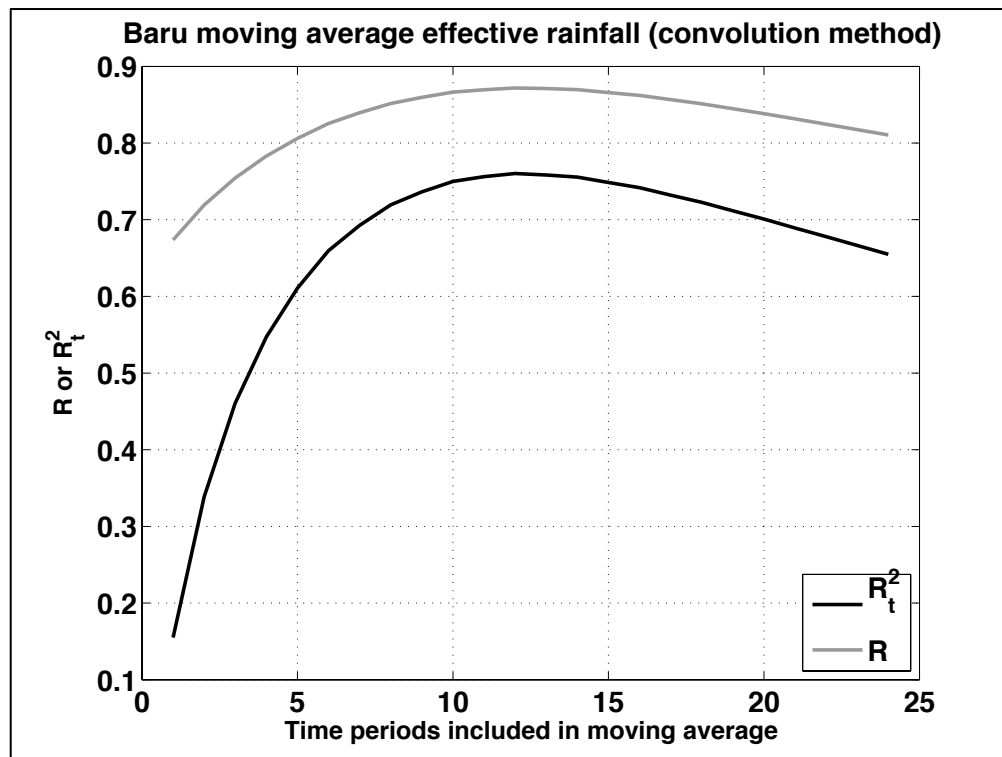
410 Figure 4 – The R_t^2 and R tend to a maximum value as aggregation increases for a) Blind Beck and b)
 411 Baru. The resolution of the inferred effective rainfall is taken to be point at which the maximum is
 412 reached or very little change is apparent. For Blind Beck, this value is reached at 10 periods for both
 413 R_t^2 and R. The result for Baru is not quite as clear but can be estimated to be 10 periods from R and 11
 414 R_t^2 and R. The result for Baru is not quite as clear but can be estimated to be 10 periods from R and 11
 415 R_t^2 and R.

Reversing Hydrology: Temporal aggregation and catchment rainfall estimation using sub-hourly data

416 or 12 from R_t^2 though R_t^2 continues to increase up to 24 time periods perhaps due to higher variability
 417 of the rainfall.



418 a)



419 b)

420 Figure 5 – A similar plot to Figure 4 with aggregation by Moving Average for a) Blind Beck and b)
 421 Baru. Rather than reaching an asymptotic level, the R_t^2 and R values maximize at 9 time periods for
 422 Blind Beck and 12 time periods for Baru (determined graphically in Matlab). These values have been
 423 used as the estimates of the resolution of the inferred effective rainfall and agree well with the
 424 estimates made by resampling.

Reversing Hydrology: Temporal aggregation and catchment rainfall estimation using sub-hourly data

425 Table 1 – Time resolution of the inferred effective rainfall sequences estimated by both resampling and
 426 moving average methods are less than the dominant (fast) mode of the catchments and considerably
 427 less than the ‘safe’ Nyquist-Shannon limit.

428

Catchment	Sampling frequency (hours)	TC _q (hrs)	TC _s (hrs)	SFI	Nyquist-Shannon Limit (hours)	Time resolution estimates	
						Aggregation by resampling	Aggregation by Moving Average
Blind Beck	.25	6.3	22.1	47%	19.9	2.5 hours (10 time periods)	2.25 hours (9 time periods)
Baru	.083	1.1	18.7	62%	3.4	0.9 - 1 hours (11-12 time periods)	1 hour (12 time periods)

429

430 Table 1 shows that the estimated resolution of the IR sequence for Blind Beck
 431 is around 9-10 time periods (i.e. 2.25-2.5 hours) and for Baru it is 11-12 time periods
 432 (i.e. 55 mins – 1hr). Both estimates are within the Nyquist-Shannon safe sampling
 433 limit and below the fast time constant for both catchments indicating that even though
 434 resolution has been lost – the trade-off for numerical stability – the dominant mode of
 435 the rainfall-streamflow dynamics has been captured. Table 2 shows that the estimated
 436 resolution of the inferred effective rainfall for both catchments is well within the
 437 Nyquist limit and, whilst the Blind Beck resolution is within the safe limits suggested
 438 by Ljung (1999) and Young (2010), the estimated resolution for Baru is close to the
 439 fast TC and outside the suggested limits. The estimates of resolution of the inferred
 440 sequence made from the aggregation plots are not always well-defined and may be
 441 dependent on the length of record which will affect the number of aggregation periods
 442 that may be meaningfully calculated given the finite length of the data series. A
 443 better means of estimation of resolution may be achieved by examining the frequency
 444 spectra of the rainfall and streamflow sequences.

445

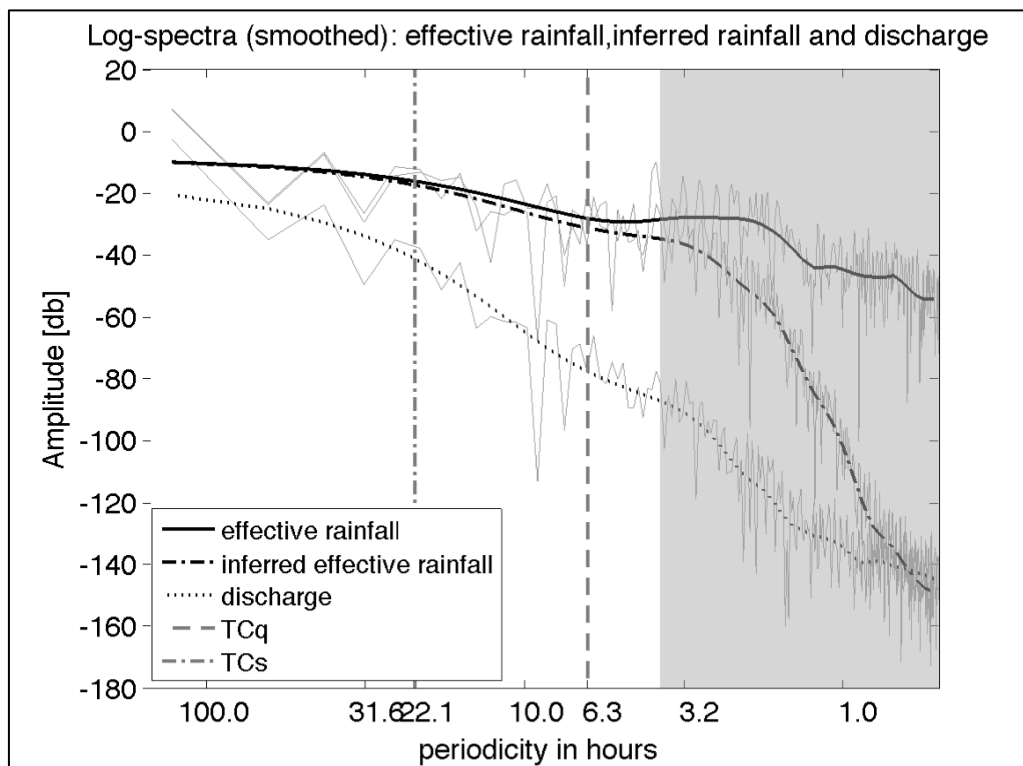
446 Table 2 – The estimated resolution of the inferred effective rainfall for Blind Beck is
 447 well within both the Nyquist limit and the safe sampling limits suggested by the
 448 Ljung (1999) and Young (2010) whereas the resolution Baru, whilst well within the

Reversing Hydrology: Temporal aggregation and catchment rainfall estimation using sub-hourly data

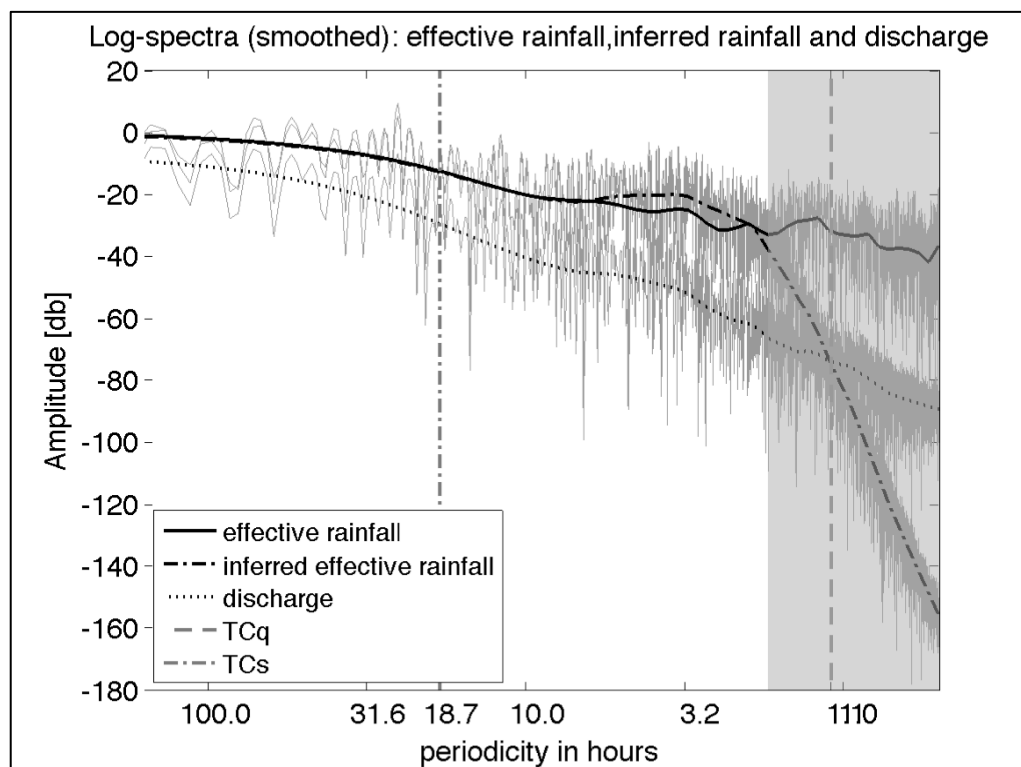
449 Nyquist limit, is close to the fast TCq and outside the suggested safe sampling limits
 450 of Ljung and Young.
 451

Catchment	TCq (hours)	Nyquist limit (hours)	Ljung interval (hours)	Young interval (hours)	Estimated resolution (hours)
Blind Beck	6.3	19.9	3.98	3.32	2.25-2.5
Baru	1.1	3.4	0.68	0.57	0.91-1.0

452
 453
 454



455 a)



456

b)

457

458

459

460

461

462

463

464

465

466

Figure 6 – Periodograms for a) Blind Beck and b) Baru showing the frequency structure of the effective rain, inferred effective rain and streamflow sequences. Both catchments show a similarity in the frequency spectra of effective and inferred effective rainfall within the catchment system. The inferred effective rainfall spectrum is very close to the actual effective rainfall one within a wide range of frequencies mostly covering those corresponding to the catchment’s time constants. There is also a strong low pass filtering effect cutting off high frequencies with low amplitudes instead of boosting this high frequency noise.

467

468

469

470

471

472

473

474

475

476

In Figure 6, the amplitude spectra of inferred effective and observed effective rainfall are very close (overlapping when smoothed) within a broad range of frequencies. The cut-off frequency, where the difference between the smoothed ER and IR spectra is approximately -6Db, provides a frequency domain estimate of the resolution. The cut-off period for Blind Beck is 3.8 hours and for Baru is 1.7 hours. For frequencies above this value, a very strong low pass filtering effect shown is by the rapid decrease in the IR spectrum. The frequency range beyond the cut-off point, shaded in Fig. 6, carries a very small proportion of the power of the signal and can be considered non-significant.

475

476

The processes and characteristics limiting the inferred effective rainfall accuracy include the slow components of the catchment dynamics and the rainfall

477 regime. These can be seen as the ‘usual suspects’ affecting the inversion process. The
478 general goodness of fit of the initial catchment model (rainfall-streamflow) appears to
479 be a factor as well, indicating that the inferred effective rainfall estimation method
480 presented here can be used to assess the quality of available data and the degree to
481 which the data characterise the catchment.

482 **Conclusions**

483 A combination of time and frequency domain techniques have been used to show that
484 the inferred effective rainfall time-series generated by the RegDer inversion method
485 does indeed approximate the direct inverse of a transfer function to a high degree of
486 accuracy within the frequency range which includes the dominant modes of the
487 rainfall-streamflow dynamics. The direct inverse exaggerates low-amplitude high
488 frequency noise, which is filtered out by the regularisation process involved in the
489 RegDer method. The smoothing of the signal resulting from regularisation is
490 quantified in the time-domain by comparison with aggregated observed input data
491 using standard model fit measures - coefficient of determination, R_t^2 , and correlation
492 coefficient, R - and analysed as a low-pass filtering process in the frequency domain.

493 **Acknowledgements**

494 The authors would like to thank Mary Ockenden for the collection and
495 quality assurance of the period of rainfall and streamflow for the Blind Beck
496 catchment (NERC grant number NER/S/A/2006/14326), and also Jamal Mohd
497 Hanapi and Johnny Larenus for the collection of the period of rainfall and streamflow
498 utilised for the Baru catchment and to Paul McKenna for its quality assurance (NERC
499 grant number GR3/9439). This work has been partly supported by the Natural
500 Environment Research Council [Consortium on Risk in the Environment:

Reversing Hydrology: Temporal aggregation and catchment rainfall estimation using sub-hourly data

501 Diagnostics, Integration, Benchmarking, Learning and Elicitation (CREDIBLE)]

502 grant number: NE/J017299/1.

503

504

505 **References**

- 506 Andrews, F., Croke, B., Jeanes, K., 2010 Robust estimation of the total unit
507 hydrograph. In: *2010 International Congress on Environmental Modelling and*
508 *Software Modelling for Environment's Sake. Ottawa, Canada.*
- 509 Beven, K.J., 2006 A manifesto for the equifinality thesis. *J. Hydrol.* 320, 18-36.
- 510 Beven, K.J., 2012 *Rainfall-Runoff Modelling - the Primer*, second ed. John Wiley and
511 Sons, Chichester, England.
- 512 Bidin, K., Chappell, N., 2003 First evidence of a structured and dynamic spatial
513 pattern of rainfall within a small humid tropical catchment. *Hydrol. Earth Syst. Sci.* 7
514 (2), 245-253.
- 515 Bidin, K., Chappell, N., 2006 Characteristics of rain events at an inland locality in
516 Northeastern Borneo, Malaysia. *Hydrol. Process.* 20 (18), 3835-3850.
- 517 Bloomfield, P. 1976 *Fourier Analysis of Time Series: An Introduction*, John Wiley &
518 Sons, New York.
- 519 Blöschl, G. (Editor), Sivapalan, M. (Editor), Wagener, T. (Editor), Viglione,
520 A. (Editor), Savenije, H. (Editor), 2013 *Runoff prediction in ungauged basins:*
521 *synthesis across processes, places and scales*, Cambridge University Press
- 522 Boorman, D. 1989 A new approach to Unit Hydrograph Modelling. *PhD Lancaster*
- 523 Brocca, L., Moramarco, T., Melone, F., & Wagner, W. 2013 A new method for
524 rainfall estimation through soil moisture observations. *Geophysical Research*
525 *Letters*, 40(5), 853-858.
- 526 Brocca, L., Ciabatta, L., Massari, C., Moramarco, T., Hahn, S., Hasenauer, S., Kidd,
527 R., Dorigo, W., Wagner, W., Levizzani, V., 2014 Soil as a natural rain gauge:
528 Estimating global rainfall from satellite soil moisture data. *Journal of Geophysical*
529 *Research: Atmospheres*, 119(9), 5128-5141.

Reversing Hydrology: Temporal aggregation and catchment rainfall estimation using sub-hourly data

- 530 Chapman T. G. 1996 Common unitgraphs for sets of runoff events: Part 2.
- 531 Comparisons and inferences for rainfall loss models. *Hydrological*
- 532 *Processes*, **10**:783–792
- 533 Chappell, N., Franks, S., Larenus, J., 1998 Multi-scale permeability estimation for a
- 534 tropical catchment. *Hydrol. Process.* 12 (9), 1507-1523.
- 535 Chappell, N.A., Tych, W., Chotai, A., Bidin, K., Sinun, W., Chiew, T.H., 2006
- 536 Barumodel: combined data based mechanistic models of runoff response in a
- 537 managed rainforest catchment. *For. Ecol. Manag.* 224 (1), 58-80.
- 538 Croke, B., 2006 A technique for deriving an average event unit hydrograph from
- 539 streamflow-only data for ephemeral quick-flow-dominant catchments. *Adv.*
- 540 *Water Resour.* 29 (4), 493-502.
- 541 Clark, M. P., and D. Kavetski 2010 Ancient numerical demons of conceptual
- 542 hydrological modeling: 1. Fidelity and efficiency of time stepping schemes, *Water*
- 543 *Resour. Res.*, 46, W10510, doi:10.1029/2009WR008894
- 544 Cuchi, J., Chinarro, D., Villarroel, J., Antonio Cuchi, D., & Luis Villarroel, J.
- 545 2014 Linear system techniques applied to the Fuenmayor Karst Spring, Huesca
- 546 (Spain). *Environmental Earth Sciences*, 71(3), 1049-1060.
- 547 Duband, D., Obléd, C., Rodriguez, J.-Y., 1993, Unit hydrograph revisited: an alternative
- 548 approach to UH and effective precipitation identification, *Journal of Hydrology*, 150,
- 549 115-149
- 550 Holman-Dodds, J. K., Bradley, A. A. and Sturdevant-Rees, P. L., 1999 Effect of
- 551 temporal sampling of precipitation on hydrologic model calibration, *Journal of*
- 552 *Geophysical Research*, Vol. 104, No. D16, Pages 19,645-19,654

Reversing Hydrology: Temporal aggregation and catchment rainfall estimation using sub-hourly data

- 553 Jakeman, A.J., Littlewood, I.G., Whitehead, P.G., 1990. Computation of the
554 instantaneous unit hydrograph and identifiable component flows with application to
555 two small upland catchments. *Journal of Hydrology* 117, 275-300.
- 556 Kavetski, D., and M. P. Clark 2010 Ancient numerical demons of conceptual
557 hydrological modelling: 2. Impact of time stepping schemes on model analysis
558 and prediction, *Water Resour. Res.*, 46, W10511, doi:10.1029/2009WR008896
- 559 Kirchner, J., 2009 Catchments as simple dynamical systems: catchment
560 characterization, rainfall-runoff modelling, and doing hydrology backward.
561 *Water Resour. Res.* 45.
- 562 Krajewski, W. F., Lakshmi, V., Georgakakos, K. P., & Jain, S. C. 1991 A Monte
563 Carlo study of rainfall sampling effect on a distributed catchment model. *Water
564 Resources Research*, 27 (1), 119-128.
- 565 Kretzschmar, A., Tych, W and Chappell, N. A. 2014 Reversing hydrology:
566 Estimation of sub-hourly rainfall time-series from streamflow. *Environmental
567 Modelling & Software* 60: 290-301.
- 568 Krier, R., Matgen, P., Goergen, K., Pfister, L., Hoffmann, L., Kirchner, J.W.,
569 Uhlenbrook, S., Savenije, H.H.G., 2012 Inferring catchment precipitation by doing
570 hydrology backward: a test in 24 small and mesoscale catchments in Luxembourg.
571 *Water Resour. Res.* 48, W10525.
- 572 Littlewood, I. G. 2007 Rainfall–streamflow models for ungauged basins:
573 uncertainty due to modelling time step. In: *Uncertainties in the ‘Monitoring–
574 Conceptualisation– Modelling’ Sequence of Catchment Research (Proc.
575 Eleventh Biennial Conference of the Euromediterranean Network of
576 Experimental and Representative Basins)* (L. Pfister & L. Hoffmann, eds),

- 577 149–155. Paris: UNESCO Tech. Doc. in Hydrology Series 81.
- 578 Littlewood, I.G. and Croke, B.F.W. 2008 Data time-step dependency of
579 conceptual rainfall—streamflow model parameters: an empirical study with
580 implications for regionalisation, *Hydrological Sciences Journal*, 53:4, 685-695,
581 DOI: 10.1623/hysj.53.4.685
- 582 Littlewood, I. G., Young, P. C. and Croke, B. F. W. 2010 Preliminary
583 comparison of two methods for identifying rainfall–streamflow model
584 parameters insensitive to data time-step: the Wye at Cefn Brwyn, Plynlimon,
585 Wales. In: *Proceedings of the Third International Symposium (British
586 Hydrological Society, 19–23 July 2010, Newcastle University, UK).*
- 587 Littlewood, I.G. and Croke, B.F.W. 2013 Effects of data time-step on the
588 accuracy of calibrated rainfall-streamflow model parameters: practical aspects
589 of uncertainty reduction, *Hydrology Research*, 44.3
- 590 Ljung, L. 1999. *System identification. Theory for the user*. Prentice Hall, Upper
591 Saddle River, 2nd edition.
- 592 Mayes, W.M., Walsh, C.L., Bathurst, J.C., Kilsby, C.G., Quinn, R.F., Wilkinson,
593 M.E., Daugherty, A.J., Connell, P.E., 2006 Monitoring a flood event in a densely
594 instrumented catchment, the Upper Eden, Cumbria, UK. *Water Environ. J.* 20 (4),
595 217-226.
- 596 Montanari, A., and E. Toth 2007 Calibration of hydrological models in the spectral
597 domain: An opportunity for scarcely gauged basins?, *Water Resour. Res.*, 43,
598 W05434, doi:10.1029/2006WR005184.
- 599 Ockenden, M.C., Chappell, N.A., 2011 Identification of the dominant runoff
600 pathways from data-based mechanistic modelling of nested catchments in temperate

Reversing Hydrology: Temporal aggregation and catchment rainfall estimation using sub-hourly data

- 601 UK. *J. Hydrol.* 402 (1), 71-79.
- 602 Ockenden, M.C., Chappell, N.A., Neal, C., 2014 Quantifying the differential
603 contributions of deep groundwater to streamflow in nested basins, using both water
604 quality characteristics and water balance. *Hydrol. Res.* 45, 200-212.
- 605 Olivera, F., Maidment, D., 1999 Geographical information systems (GIS)- based spatially
606 distributed model for runoff routing, *Water Resources Research*, 35, 1155-1164
- 607 Reynard, N.S., Stewart, E.J., 1993 The derivation of design rainfall profiles for
608 upland areas of the UK. *Meteorol. Mag.* 122, 116-123.
- 609 Szolgayová, E.,; Arlt, J., Blöschl, G., Szolgay, J. 2014 Wavelet based
610 deseasonalization for modelling and forecasting of daily streamflow series
611 considering long range dependence. *Journal of Hydrology and Hydromechanics*, 62
612 (1). pp. 24-32. ISSN 0042-790X
- 613 Taylor, C.J., Pedregal, D.J., Young, P.C., Tych, W., 2007 Environmental time series
614 analysis and forecasting with the Captain toolbox. *Environ. Model. Softw.* 22 (6), 797-
615 814.
- 616 Teuling, A.J., Lehner, I., Kirchner, J.W., Seneviratne, S.I., 2010 Catchments as
617 simple dynamical systems: experience from a Swiss pre-alpine catchment. *Water*
618 *Resour. Res.* 46 (10).
- 619 Wickert, M., 2013 *Signals and Systems for Dummies*, 1st Edition, John Wiley &
620 Sons;
- 621 Young, P.C. 2010 The estimation of continuous-time rainfall–flow models for flood
622 risk management. In: *Proceedings of the Third International Symposium (British*
623 *Hydrological Society, 19–23 July 2010, Newcastle University, UK).*
- 624 Young, P.C. and Beven, K.J., 1994 Data-based mechanistic modelling and the
625 rainfall-flow non-linearity, *Environmetrics*, 5, 335-363

Reversing Hydrology: Temporal aggregation and catchment rainfall estimation
using sub-hourly data

- 626 Young, P.C., Garnier, H., 2006 Identification and estimation of continuous-time, data-
627 based mechanistic (DBM) models for environmental systems. *Environ. Model. Softw.*
628 21 (8), 1055-1072.
- 629 Young, P.C., Sumińska, M.A., 2012. Control systems approach to input estimation
630 with hydrological applications. In: *16th IFAC Symposium on System Identification.*
631 *July 2012, Brussels, Belgium, pp. 1043-1048.*
- 632 Young, P.C., Pedregal, D.J., Tych, W., 1999 Dynamic harmonic regression. *J.*
633 *Forecast.* 18 (6), 369-394.
- 634